

# Gravitational collapse with tachyon field and barotropic fluid

Y. Tavakoli,<sup>1,\*</sup> J. Marto,<sup>1,†</sup> A. H. Ziaie,<sup>2,‡</sup> and P. V. Moniz<sup>1,3,§</sup>

<sup>1</sup>*Departamento de Física, Universidade da Beira Interior, 6200 Covilhã, Portugal*

<sup>2</sup>*Department of Physics, Shahid Beheshti University, Evin, 19839 Tehran, Iran*

<sup>3</sup>*CENTRA, IST, Av. Rovisco Pais, 1, Lisboa, Portugal*

(Dated: 5th November 2018)

A particular class of space-time, with a tachyon field,  $\phi$ , and a barotropic fluid constituting the matter content, is considered herein as a model for gravitational collapse. For simplicity, the tachyon potential is assumed to be of inverse square form *i.e.*,  $V(\phi) \sim \phi^{-2}$ . Our purpose, by making use of the specific kinematical features of the tachyon, which are rather different from a standard scalar field, is to establish the several types of asymptotic behavior that our matter content induces. Employing a dynamical system analysis, complemented by a thorough numerical study, we find classical solutions corresponding to a naked singularity or a black hole formation. In particular, there is a subset where the fluid and tachyon participate in an interesting tracking behaviour, depending sensitively on the initial conditions for the energy densities of the tachyon field and barotropic fluid. Two other classes of solutions are present, corresponding respectively, to either a tachyon or a barotropic fluid regime. Which of these emerges as dominant, will depend on the choice of the barotropic parameter,  $\gamma$ . Furthermore, these collapsing scenarios both have as final state the formation of a black hole.

PACS numbers: 04.20.Dw, 04.70.Bw, 04.20.Cv, 97.60.Lf

## I. INTRODUCTION

The study of the final state of the gravitational collapse of initially regular distributions of matter is one of the open problems in classical general relativity, having attracted remarkable attention in past decades. When a sufficiently massive star exhausts all the thermonuclear sources of its energy, it would undergo a collapsing scenario due to its own gravity, without reaching a final state in terms of a neutron star or white dwarf. Under a variety of circumstances, singularities will inevitably emerge (geodesic incompleteness in space-time), matter densities and space-time curvatures diverging. Albeit the singularity theorems [1, 2] state that there exist space-time singularities in a generic gravitational collapse, they provide no information on the nature of singularities: the problem of whether these regions are hidden by a space-time event horizon or can actually be observed, remains unsolved. The cosmic censorship conjecture (CCC), as hypothesized by Penrose [3], conveys that the singularities appearing at the collapse final outcome must be hidden within an event horizon and thus no distant observer could detect them. A black hole forms. Although the CCC plays a crucial role in the physics of black holes, there is yet no proof of it, due to the lack of adequate tools to treat the global characteristics of the field equations. Nevertheless, in the past 30 years many solutions to the field equations have been discovered, which exhibit the occurrence of naked singularities, where the matter content has included perfect and imperfect fluids [4, 5], scalar fields [6], self-similar models [7] and null strange quarks [8]. Basically, it is the geometry of trapped surfaces that decides the visibility or otherwise of the space-time singularity. In case the collapse terminates into a naked singularity, the trapped surfaces do not emerge early enough, allowing (otherwise hidden) regions to be visible to the distant observers.

The gravitational collapse of scalar fields is of relevance [9], owing to the fact that they are able to mimic other types of behaviours, depending on the choice of the potentials. Scalar field models have been extensively examined for studying CCC in spherically symmetric models [10], non-spherically symmetric models [11] and also for static cases [12]. Their role in understanding the machinery governing the causal structure of space-time was available since the 90's, when the numerical solutions exhibiting naked singularities were found numerically by Choptuik [13] and analytically by Christodoulou [14]. There are in the literature a few papers discussing gravitational collapse in the presence of a scalar field joined by a fluid for the matter content [15, 16]: in summary, a black hole forms in these collapsing situations. However, to our knowledge, a tachyon scalar field has not yet been considered regarding whether a black hole or naked singularity forms, that is to say, in the CCC context, together with a fluid. Tachyon fields arise in

---

\*Electronic address: tavakoli@ubi.pt

†Electronic address: jmarto@ubi.pt

‡Electronic address: ahziaie@sbu.ac.ir

§Electronic address: pmoniz@ubi.pt

the framework of string theory [17] and have been of recent use in cosmology [18]. The action for the tachyon field has a non-standard kinetic term [19], enabling for several effects whose dynamical consequences are different from those of a standard scalar field [20]. Namely, other (anti-)friction features that can alter the outcome of a collapsing scenario. This constitutes a worthy motivation to investigate the scenario where a tachyon field is added to a barotropic fluid, both constituting the matter content present in the collapse process: on the one hand, the fluid will play the role of conventional matter from which a collapse can proceed into, whereas, on the other hand, the tachyon would convey, albeit by means of a simple framework, some intrinsic features from a string theory setting. Restricting ourselves herein to the tachyon as the intrinsic string ingredient influencing the collapse, let us nevertheless point that many other string features could be incorporated in subsequent similar studies [9, 17, 19]. Our purpose, in this paper, by investigating the gravitational collapse of a barotropic fluid together with a tachyon field, is therefore to establish the types of final state that can occur (i.e., whether a black hole or a naked singularity emerges, in the context of the CCC), which matter component will determine the outcome. In particular, if the late time tachyon behaviour, possibly competing with the fluid and eventually becoming dominant, could allow interesting features to appear.

We then organize this paper as follows. In section II we give a brief review on the gravitational collapse of a specific space-time, namely the marginally bounded case (cf. [21]). In section III we study, by means of a dynamical system analysis, the gravitational collapse employing a tachyon and a barotropic fluid as the matter content. The analytical study is complemented by a careful numerical investigation. In section IV we present our conclusions and a discussion of our results.

## II. A BRIEFING ON MARGINALLY BOUND GRAVITATIONAL COLLAPSE

In this section, we will discuss the space-time region inside the collapsing sphere which will contain the chosen matter content. An isotropic Friedmann-Robertson-Walker (FRW) metric, in comoving coordinates, will be considered as the interior space-time for the gravitational collapse. However, in order to study the whole space-time, we must match this interior region to a suitable exterior. In the model herein, it is convenient to consider a spherically symmetric and inhomogeneous space-time such as the Schwarzschild or the generalized Vaidya geometries to model the space-time outside the collapsing sphere.

The interior space-time for the marginally bounded case (cf. [21]) can be parametrized as

$$ds^2 = -dt^2 + a(t)^2 dr^2 + R(t, r)^2 d\Omega^2, \quad (2.1)$$

where  $t$  is the proper time for a falling observer whose geodesic trajectories are labeled by the comoving radial coordinate  $r$ ,  $R(t, r) = ra(t)$  is the area radius of the collapsing volume and  $d\Omega^2$  being the standard line element on the unit two-sphere. The Einstein's field equations for this model can be presented [1] as (we have set  $8\pi G = c = 1$  throughout this paper)

$$\rho = \frac{F_{,r}}{R^2 R_{,r}}, \quad p = \frac{-\dot{F}}{R^2 \dot{R}}, \quad (2.2)$$

where the mass function

$$F(t, r) = R\dot{R}^2, \quad (2.3)$$

is the total gravitational mass within the shell, labeled by the comoving radial coordinate  $r$  with “ $r \equiv \partial_r$ ” and “ $\equiv \partial_t$ ”. Since we are interested in a continuous collapsing scenario, we take  $\dot{a} < 0$ , implying that the area radius of the collapsing shell, for a constant value of  $r$ , decreases monotonically. Splitting the above metric for a two-sphere and a two dimensional hypersurface, normal to the two-sphere, we have

$$ds^2 = h_{ab} dx^a dx^b + R(t, r)^2 d\Omega^2, \quad h_{ab} = \text{diag} [-1, a(t)^2], \quad (2.4)$$

whereby the Misner-Sharp energy [22] is defined to be

$$E(t, r) = \frac{R(t, r)}{2} [1 - h^{ab} \partial_a R \partial_b R] = \frac{R\dot{R}^2}{2}. \quad (2.5)$$

To discuss the final state of gravitational collapse it is important to study the conditions under which the trapped surfaces form. From the above definition, it is the ratio  $2E(t, r)/R(t, r)$  that controls the formation of trapped surfaces

[22] (note that the mass function defined above is nothing but twice the Misner-Sharp mass). Introducing the null coordinates

$$d\xi^+ = -\frac{1}{\sqrt{2}} [dt - a(t)dr], \quad d\xi^- = -\frac{1}{\sqrt{2}} [dt + a(t)dr], \quad (2.6)$$

the metric (2.4) can be recast into the double-null form

$$ds^2 = -2d\xi^+d\xi^- + R(t,r)^2d\Omega^2. \quad (2.7)$$

The radial null geodesics are given by  $ds^2 = 0$ . We then may deduce that there exists two kinds of null geodesics which correspond to  $\xi^+ = \text{constant}$  and  $\xi^- = \text{constant}$ , the expansions of which are given by

$$\Theta_{\pm} = \frac{2}{R} \partial_{\pm} R, \quad (2.8)$$

where

$$\partial_+ = \frac{\partial}{\partial \xi^+} = -\sqrt{2} \left[ \partial_t - \frac{\partial_r}{a(t)} \right], \quad \partial_- = \frac{\partial}{\partial \xi^-} = -\sqrt{2} \left[ \partial_t + \frac{\partial_r}{a(t)} \right]. \quad (2.9)$$

The expansion parameter measures whether the bundle of null rays normal to the sphere is diverging ( $\Theta_{\pm} > 0$ ) or converging ( $\Theta_{\pm} < 0$ ). The space-time is referred to as trapped, untrapped and marginally trapped if

$$\Theta_+\Theta_- > 0, \quad \Theta_+\Theta_- < 0, \quad \Theta_+\Theta_- = 0, \quad (2.10)$$

respectively, where we have noted that  $h^{ab}\partial_a R \partial_b R = -\frac{R^2\Theta_+\Theta_-}{2}$ . The third case characterizes the outermost boundary of the trapped region, the apparent horizon equation being  $\dot{R}^2 = 1$ . From the point of view of equation (2.5), we see that at the boundary of the trapped region,  $2E(t,r) = R(t,r)$ . Thus, in the regions where the mass function satisfies the relation  $F(t,r) > R(t,r)$ , the trapping of light does occur, whereas for the regions in which the mass function is less than the area radius i.e.,  $F(t,r) < R(t,r)$ , no trapping happens [22]. In other words, in the former there exists a congruence of future directed null geodesics emerging from a past singularity and reaching to distant observers, causing the singularity to be exposed (a naked singularity forms). In the latter, no such families exist and trapped surfaces will form early enough before the singularity formation: regions will be hidden behind the event horizon, which lead to the formation of a black hole [1] (a similar interpretation has been given in [23, 24]).

In order to further illustrate this specific gravitational collapse process, let us employ a very particular class of solutions. We assume that the behavior of the matter density, for  $a \ll 1$ , is given by the following ansatz<sup>1</sup> (cf. ref. [25, 26]),

$$\rho(t) \approx \frac{c}{a^n}, \quad (2.11)$$

where  $c$  and  $n$  are positive constants<sup>2</sup>. Integration of the first equation in (2.2) gives the following relation for the mass function as

$$F = \frac{1}{3}\rho(t)R^3. \quad (2.13)$$

Hence we have

$$\frac{F}{R} = \frac{c}{3}r^2a^{2-n}. \quad (2.14)$$

It is therefore possible to identify the following outcomes:

<sup>1</sup> Notice that, since the interior space-time (2.4) is spatially homogeneous, it is obvious that, the energy-momentum tensor must also be spatially homogeneous.

<sup>2</sup> Using the energy density (2.11) and pressure (2.15), the weak energy condition can be written as follows

$$\rho + p = \frac{nc}{3a^n} > 0. \quad (2.12)$$

The weak energy condition is satisfied throughout the collapse process (see also next section for more details regarding the issue of the energy conditions).

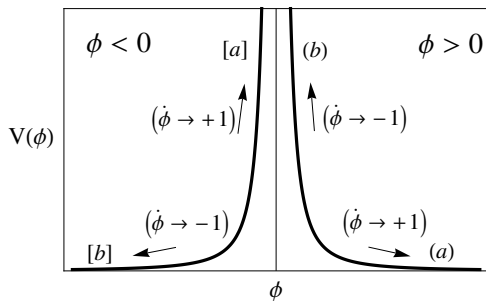


Figure 1: The potential  $V = V_0\phi^{-2}$ , denoting the  $\phi < 0$  and  $\phi > 0$  branches as well as the asymptotic stages.

- For  $0 < n < 2$ , the ratio  $F/R < 1$  is less than unity throughout the collapse and if no trapped surfaces exist initially, due to the regularity condition ( $F(t_0, r)/R(t_0, r) < 1$  for a suitable value of  $c$  and  $r$ ), then no trapped surfaces would form until the epoch  $a(t_s) = 0$ . More precisely, there exists a family of radial null trajectories emerging from a naked singularity.
- For  $n \geq 2$ , the ratio  $F/R$  goes to infinity and trapped surfaces will form as the collapse evolves, which means that singularity will be covered and no radial geodesics can emerge from it. Thus, a black hole forms.

From equation (2.11), we may easily find a relation between the energy density and pressure as

$$p = \frac{n-3}{3}\rho, \quad (2.15)$$

which shows that for  $n < 2$ , where a naked singularity occurs, the pressure gets negative values [27]. From equations (2.3), (2.11) and bearing in mind the continuous collapse process ( $\dot{a} < 0$ ) we can solve for the scale factor as

$$a(t) = \left( a_0^{\frac{n}{2}} + \frac{n}{2} \sqrt{\frac{c}{3}} (t_0 - t) \right)^{\frac{2}{n}}, \quad (2.16)$$

where  $t_0$  is the time at which the energy density begins increasing as  $a^{-n}$  and  $a_0$  corresponds to  $t_0$ . Assuming that the collapse process initiates at  $t_0 = 0$ , the time at which the scale factor vanishes corresponds to  $t_s = \frac{2}{n} \sqrt{\frac{3}{c}} a_0^{n/2}$ , implying that the collapse ends in a finite proper time.

### III. GRAVITATIONAL COLLAPSE WITH TACHYON AND BAROTROPIC FLUID

The model we employ to study the gravitational collapse has an interior space-time geometry as described above (see e.g. [1, 21, 28]). Concerning the matter content, we consider a spherically symmetric homogeneous tachyon field together with a barotropic fluid. We use an inverse square potential for the tachyon field given by [29–31],

$$V(\phi) = V_0\phi^{-2}, \quad (3.1)$$

where  $V_0$  is a constant. Note that we can consider the potential (3.1) as two (mirror) branches (see figure 1), upon the symmetry  $\phi \rightarrow -\phi$ , treating the  $\phi > 0$  and  $\phi < 0$  separately.

The total energy density of the collapsing system is therefore  $\rho = \rho_\phi + \rho_b$ , with

$$\rho = 3H^2 = \frac{V(\phi)}{\sqrt{1-\dot{\phi}^2}} + \rho_b, \quad (3.2)$$

where  $\rho_b$  is the energy density of the barotropic matter, whose pressure  $p_b$ , in terms of the barotropic parameter,  $\gamma$ , satisfies the relation  $p_b = (\gamma - 1)\rho_b$ , the barotropic parameter being positive,  $\gamma > 0$ . Then, the Raychadhuri equation for the collapsing system can be written as

$$-2\dot{H} = \frac{V(\phi)\dot{\phi}^2}{\sqrt{1-\dot{\phi}^2}} + \gamma\rho_b. \quad (3.3)$$

Furthermore, the equation of motion for the tachyon field can be obtained as

$$\ddot{\phi} = -(1 - \dot{\phi}^2) \left[ 3H\dot{\phi} + \frac{V_{,\phi}}{V} \right]. \quad (3.4)$$

The energy conservation of the barotropic matter is

$$\dot{\rho}_b + 3\gamma H \rho_b = 0. \quad (3.5)$$

Integrating (3.5), the energy density for barotropic matter can be presented as  $\rho_b = \rho_{0b} a^{-3\gamma}$ , where  $\rho_{0b}$  is a constant of integration. The total pressure is given by

$$p = p_\phi + (\gamma - 1)\rho_{0b} a^{-3\gamma}. \quad (3.6)$$

In order to have a physically reasonable matter content for the collapsing cloud, the tachyon field and the barotropic fluid would have to satisfy the weak and dominant energy conditions<sup>3</sup> [1, 2, 36]: for any time-like vector  $V^i$ , the energy-momentum tensor  $T_{ik}$  satisfies  $T_{ik}V^iV^k \geq 0$  and  $T^{ik}V_k$  must be non-space-like. Since for the symmetric metric (2.1) we have  $T^t_t = -\rho(t)$  and  $T^r_r = T^\theta_\theta = T^\varphi_\varphi = p(t)$ , then, for the energy densities and the pressures of the tachyon field and the barotropic fluid the energy conditions amount to the following relations

$$\rho_\phi \geq 0, \quad \rho_\phi + p_\phi \geq 0, \quad |p_\phi| \leq \rho_\phi, \quad (3.7)$$

$$\rho_b \geq 0, \quad \rho_b + p_b \geq 0, \quad |p_b| \leq \rho_b. \quad (3.8)$$

The first two expressions in equations (3.7) and (3.8) denote the ‘weak energy condition’ (WEC), and the last expression denotes the ‘dominant energy condition’ (DEC).

For a tachyon field, it is straightforward to show that the WEC is satisfied:

$$\rho_\phi = \frac{V(\phi)}{\sqrt{1 - \dot{\phi}^2}} \geq 0, \quad \text{and} \quad \rho_\phi + p_\phi = \frac{V\dot{\phi}^2}{\sqrt{1 - \dot{\phi}^2}} \geq 0. \quad (3.9)$$

In addition, since  $\dot{\phi}^2 < 1$ , then  $V(\phi)(1 - \dot{\phi}^2)^{-1/2} \geq V(\phi)\sqrt{1 - \dot{\phi}^2}$  from which it follows that  $|p_\phi| \leq \rho_\phi$ , and hence, the DEC is satisfied for the tachyon matter.

For the barotropic fluid considered herein, we assume a regular initial condition for the collapsing system, such as  $\rho_{0b} > 0$ , indicating that  $\rho_b = \rho_{0b} a^{-3\gamma} > 0$ . In addition, since  $p_b = (\gamma - 1)\rho_b$ , then  $p_b + \rho_b = \gamma\rho_b \geq 0$  provided that  $\gamma > 0$ ; through this paper we will consider the positive barotropic parameter  $\gamma$ . Hence, the WEC is satisfied. On the other hand, considering the DEC ( $\rho_b \geq |p_b|$ ) it follows that the barotropic parameter  $\gamma$  must satisfy the range  $\gamma \leq 2$  (cf. the phase space analysis in section III A).

### A. Phase space analysis

We analyze in this (sub)section the gravitational collapse of the above setup by employing a dynamical system perspective. We introduce a new time variable  $\tau$  (instead of the proper time  $t$  present in the comoving coordinate system  $\{t, r, \theta, \varphi\}$ ), defined as

$$\tau \equiv -\log\left(\frac{a}{a_0}\right)^3, \quad (3.10)$$

where  $0 < \tau < \infty$  (the limit  $\tau \rightarrow 0$  corresponds to an initial condition of the collapsing system ( $a \rightarrow a_0$ ) and the limit  $\tau \rightarrow \infty$  corresponds to  $a \rightarrow 0$ ). For any time dependent function  $f = f(t)$ , we can therefore write<sup>4</sup>

$$\frac{df}{d\tau} \equiv -\frac{\dot{f}}{3H}, \quad (3.11)$$

<sup>3</sup> We note that satisfying the weak energy condition implies that the null energy condition (NEC) is held as well.

<sup>4</sup> We recall that throughout this paper  $H < 0$ , i.e.,  $\dot{a} < 0$  is assumed.

We further introduce a new set of dynamical variables  $x$ ,  $y$  and  $s$  as follows [20]

$$x \equiv \dot{\phi}, \quad y \equiv \frac{V}{3H^2}, \quad s \equiv \frac{\rho_b}{3H^2}. \quad (3.12)$$

From the new variables (3.11), (3.12) and the system (3.3)-(3.5) with (3.1), an autonomous system of equations is retrieved:

$$\frac{dx}{d\tau} \equiv f_1 = \left( x - \frac{\lambda}{\sqrt{3}}\sqrt{y} \right) (1 - x^2), \quad (3.13)$$

$$\frac{dy}{d\tau} \equiv f_2 = -y \left[ x \left( x - \frac{\lambda}{\sqrt{3}}\sqrt{y} \right) + s(\gamma - x^2) \right], \quad (3.14)$$

$$\frac{ds}{d\tau} \equiv f_3 = s(1 - s)(\gamma - x^2). \quad (3.15)$$

Note that  $\lambda$  is given by

$$\lambda \equiv -\frac{V_{,\phi}}{V^{3/2}}, \quad (3.16)$$

which for the potential (3.1) brings  $\lambda = \pm 2/\sqrt{V_0}$  as a constant; for the  $\phi > 0$  branch,  $\lambda > 0$ , and for  $\phi < 0$  branch,  $\lambda < 0$ . Equation (3.2) in terms of the new variables reads<sup>5</sup>,

$$\frac{y}{\sqrt{1 - x^2}} + s = 1. \quad (3.17)$$

The dynamical variables have the range  $y > 0$ ,  $s \leq 1$ , and  $-1 < x < 1$ . This brings an effective two-dimensional phase space<sup>6</sup>.

Setting  $(f_1, f_2, f_3)|_{(x_c, y_c, s_c)} = 0$ , we can obtain the critical points  $(x_c, y_c, s_c)$  for the autonomous system. The stability can be subsequently discussed by using the eigenvalues of the Jacobi matrix  $\mathcal{A}$ , defined at each fixed point  $(x_c, y_c, s_c)$ , as

$$\mathcal{A} = \begin{pmatrix} \frac{\partial f_1}{\partial x} & \frac{\partial f_1}{\partial y} & \frac{\partial f_1}{\partial s} \\ \frac{\partial f_2}{\partial x} & \frac{\partial f_2}{\partial y} & \frac{\partial f_2}{\partial s} \\ \frac{\partial f_3}{\partial x} & \frac{\partial f_3}{\partial y} & \frac{\partial f_3}{\partial s} \end{pmatrix} \Big|_{(x_c, y_c, s_c)}. \quad (3.18)$$

Solutions, in terms of the dynamical variables, in the neighborhood of a critical point  $q_i^{\text{crit}}$  can be extracted by making use of

$$q_i(t) = q_i^{\text{crit}} + \delta q_i(t), \quad (3.19)$$

with the perturbation  $\delta q_i$  given by

$$\delta q_i = \sum_j^k (q_0)_i^j \exp(\zeta_j N), \quad (3.20)$$

where  $q_i \equiv \{x, y, s\}$ ,  $\zeta_j$  are the eigenvalues of the Jacobi matrix, and the  $(q_0)_i^j$  are constants of integration. We have summarized the fixed points for the autonomous system and their more relevant stability properties in table I.

Table I is complemented with figure 2. The autonomous system equations (3.13)-(3.15) unfolds a three dimensional phase space constrained by (3.17). Therefore the main fixed points (and the trajectories nearby) are located on surfaces of this three dimensional phase space. Furthermore, from table I, we can focus our attention on three situations characterized by having  $s = 0$ ,  $s = 1$  and  $s = s_0$ . Briefly, in more detail:

<sup>5</sup> Or equivalently, the surface where the trajectories will be present can be written as  $y^2 = (1 - s)^2 (1 - x^2)$ .

<sup>6</sup> In the absence of a barotropic fluid, the effective phase space is one-dimensional.

point	$x$	$y$	$s$	Existence	Stability
$(a)$ , $[a]$	1	0	0	for all $\lambda$ ; $\gamma < 1$	Stable node
$(b)$ , $[b]$	-1	0	0	for all $\lambda$ ; $\gamma > 1$	Saddle point
$(c)$ , $[c]$	$-\frac{\lambda}{\sqrt{3}}\sqrt{y_0}$	$y_0$	0	for all $\lambda$ ; $\gamma < 1$	Stable node
				for all $\lambda$ ; $\gamma > 1$	Saddle point
$(d)$ , $[d]$	0	0	1	for all $\lambda$ ; $\gamma \leq \gamma_1$	Unstable node
				for all $\lambda$ ; $\gamma \neq 0$	Saddle point
$(e)$	$-\sqrt{\gamma}$	$\frac{3\gamma}{\lambda^2}$	$s_0$	$\lambda > 0$ , $\gamma < \gamma_1 < 1$	Unstable node
$[e]$	$\sqrt{\gamma}$	$\frac{3\gamma}{\lambda^2}$	$s_0$	$\lambda < 0$ , $\gamma < \gamma_1 < 1$	Unstable node
$(f)$ , $[f]$	1	0	1	for all $\lambda$ ; $\gamma > 1$	Stable node
				for all $\lambda$ ; $\gamma < 1$	Saddle point
$(g)$ , $[g]$	-1	0	1	for all $\lambda$ ; $\gamma > 1$	Stable node
				for all $\lambda$ ; $\gamma < 1$	Saddle point
$(h)$ , $[h]$	1	0	$s_1$	$\gamma = 1$	Stable node
$(i)$ , $[i]$	-1	0	$s_1$	$\gamma = 1$	Stable node

Table I: Summary of critical points and their properties for the  $\phi < 0$  (denoted with square brackets, i.e., as, for example,  $[a]$ ) and  $\phi > 0$  branches (denoted with regular brackets, i.e., as, for example,  $(a)$ ).

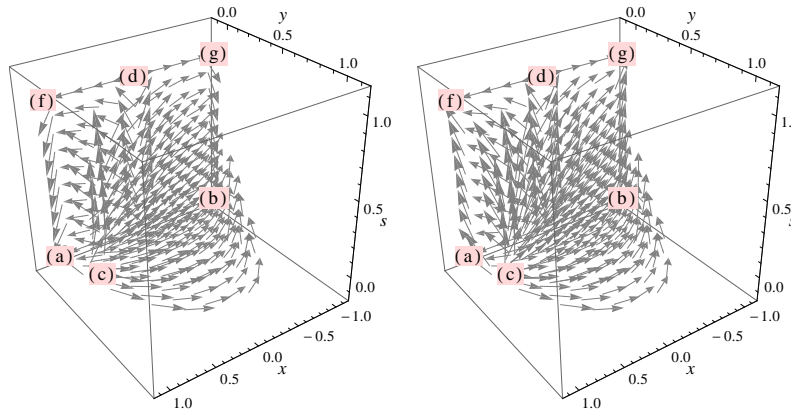


Figure 2: Trajectories in phase space and critical points: (i) Left plot represents the phase space region  $(x, y, s)$  constrained by (3.17). Therein we also depicted all the fixed points (see table I), except point  $(e)$ , for  $V_0 = 4/9$ ,  $\gamma = 0.5$ . (ii) In the right plot we considered the conditions as  $V_0 = 4/9$ ,  $\gamma = 1.5$ . We can illustrate that going from  $\gamma < 1$  to  $\gamma > 1$  (from left to the right plot) reverses the direction of the trajectories, i.e., in the left plot the vector field is directed towards points  $(a)$  or  $(b)$ . In the right plot the vector field is directed towards points  $(f)$  or  $(g)$ .

- **Point  $(a)$ :** The eigenvalues are  $\zeta_1 = -2$ ,  $\zeta_2 = -1$  and  $\zeta_3 = (\gamma - 1)$ . For  $\gamma < 1$ , all the characteristic values are real and negative, then the trajectories in the neighborhood of this point are attracted towards it. Hence,  $(a)$  is a stable node (attractor). Finally, for  $\gamma > 1$ , all characteristic values are real, but one is positive and two are negative, the trajectories approach this point on a surface and diverge along a curve: this is a saddle point.
- **Point  $(b)$ :** The eigenvalues are  $\zeta_1 = -2$ ,  $\zeta_2 = -1$  and  $\zeta_3 = (\gamma - 1)$ . This point has the same eigenvalues of point  $(a)$  and similar asymptotic behavior, being also a stable node for  $\gamma < 1$  (see the left plot in figure 3) and a saddle point for  $\gamma > 1$ .
- **Point  $(c)$ :** This fixed point has eigenvalues  $\zeta_1 = 0$ ,  $\zeta_2 = (\lambda^2 y_0 + 6y_0^2)/6 > 0$  and  $\zeta_3 = (\gamma - \lambda^2 y_0/3)$ , which all are real and  $y_0 = -\lambda^2/6 + \sqrt{1 + (\lambda^2/6)^2}$ . For  $\gamma > \gamma_1 \equiv \lambda^2 y_0/3$ , two components are positive. However, from a numerical investigation we can assert that this corresponds to an unstable saddle (see left plot in figure 3). On the other hand, for  $\gamma < \gamma_1$ , one component is negative and other is positive, and hence, a saddle point configuration would emerge.

- **Point (d):** The eigenvalues are  $\zeta_1 = 1$ ,  $\zeta_2 = -\gamma$  and  $\zeta_3 = -\gamma$ . As  $\gamma > 0$ , trajectories approach this point on a surface (the in-set) and diverge along a curve (the out-set). This is a saddle point (see left plot in figure 2).
- **Point (e):** This point is located at  $(-\sqrt{\gamma}, \frac{3\gamma}{\lambda^2}, s_0)$ , where  $s_0 = (1 - \frac{3\gamma}{\lambda^2\sqrt{1-\gamma}})$ . From the constraint  $0 \leq s_0 \leq 1$  we get

$$0 \leq 1 - \frac{3\gamma}{\lambda^2\sqrt{1-\gamma}} \leq 1, \quad (3.21)$$

i.e.,

$$0 \leq \gamma \leq \gamma_1 < 1. \quad (3.22)$$

When  $\gamma \rightarrow 0$ , points (e) and (d) become coincident (see table I). When we consider  $s_0 = 0$ , we obtain  $\gamma = \gamma_1$ ,  $x = -\frac{\lambda}{\sqrt{3}}\sqrt{y_0}$  and  $y = y_0$ . Consequently point (e) and (c) become coincident. Therefore, point (e) can be found along a curve that joins points (c) (on the surface with  $s = 0$ ) and (d) (on the surface with  $s = 1$ ). The eigenvalues are  $\zeta_1 = 0$ , with  $\zeta_2$  and  $\zeta_3$  given by,

$$\zeta_{2,3} = \frac{1}{4} \left( 2 - \gamma \pm \sqrt{(1-\gamma)(4-16s_0\gamma) + \gamma^2} \right). \quad (3.23)$$

The eigenvalues (3.23) are non negative for  $\gamma < \gamma_1$  and for  $\gamma = \gamma_1$ ,  $\zeta_2 > 0$  and  $\zeta_3 = 0$ .

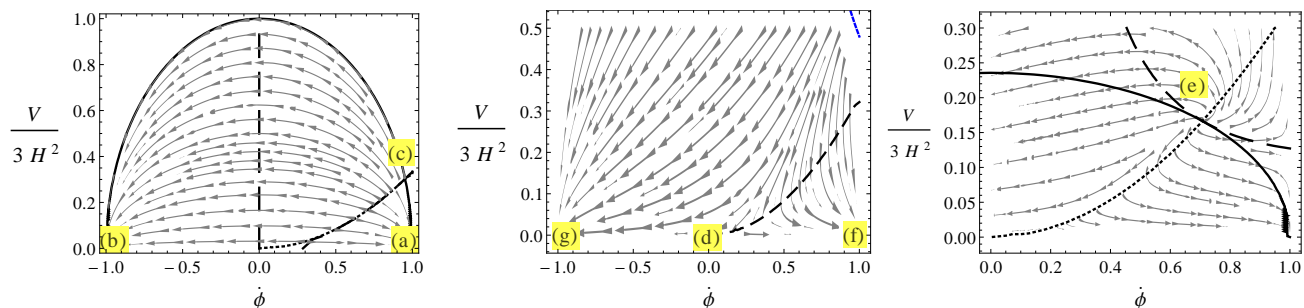


Figure 3: (i) The top left plot represents a section, of the three dimensional phase space presented in figure 2, labeled with  $s = 0$ . The dashed and dotted lines are the zeros of eqs. (3.13)-(3.15). The full line represents constraint (3.17). Therefore, the fixed points are found on their intersections. We considered the conditions as  $V_0 = 4/9$ ,  $\gamma = 0.5$ . In this example we can locate the position of fixed points (a), (b) and (c) according to table I. (ii) The center plot represents a section, showing fixed point (e), labeled with  $s = 0.76$ . The dashed (and also dotted) lines are the zeros of eqs. (3.13)-(3.15) and the full line represents constraint (3.17), as before. We considered the conditions as  $V_0 = 4/9$ ,  $\gamma = 0.5$ . (iii) Finally, in the top right plot we represent a section, labeled with  $s = 1$ . We can identify fixed points (g), (d) and (f). We considered the conditions as  $V_0 = 4/9$ ,  $\gamma = 1.2$ .

In the plot at the center of figure 3 we provide a section of the phase space showing point (e), where it can be seen that all trajectories are divergent from it. This behavior is characteristic of an unstable node and expected whenever point (e) is found along the curve that connects (c) and (d).

- **Point (f):** The eigenvalues are  $\zeta_1 = -2$ ,  $\zeta_2 = -\gamma$  and  $\zeta_3 = (1 - \gamma)$ . For  $\gamma > 1$ , all the characteristic values are real and negative, then the trajectories in the neighborhood of this point are attracted towards it. Hence, (f) is a stable node (attractor). Finally, for  $\gamma < 1$ , all characteristic values are real, but one is positive and two are negative. The trajectories approach this point on a surface and diverge along a curve; this is a saddle point.
- **Point (g):** The eigenvalues are  $\zeta_1 = -2$ ,  $\zeta_2 = -\gamma$  and  $\zeta_3 = (1 - \gamma)$ . This point has the same eigenvalues of point (f) and similar asymptotic behavior, being also a stable node for  $\gamma > 1$  (see the right plot in figure 3) and a saddle point for  $\gamma < 1$ .
- **Point (h):** This point is found along the line segment with  $x = 1$ ,  $y = 0$  and  $s \in ]0, 1[$ . The eigenvalues are  $\zeta_1 = -2$ ,  $\zeta_2 = -1$  and  $\zeta_3 = 2(s_1 - 1)$ , where  $s_1 \in ]0, 1[$ . In this case, all the characteristic values are real and negative, then the trajectories in the neighborhood of this points are attracted towards it. Hence, (h) is a stable node (attractor).



- **Point (i):** This point is found along the line segment with  $x = -1$ ,  $y = 0$  and  $s \in ]0, 1[$ . The eigenvalues are  $\zeta_1 = -2$ ,  $\zeta_2 = -1$  and  $\zeta_3 = 2(s_1 - 1)$ . This point has the same eigenvalues of point (h) and similar asymptotic behavior, being also a stable node.

Before proceeding, let us add two comments. On the one hand, note the transition that occurs, when going from  $\gamma < 1$  to  $\gamma > 1$ , an intermediate state as discussed (by means of a numerical study) in subsection III B 3. This bifurcation behaviour is made explicit through the numerical methods employed. These allowed us to confirm the results on the dynamical system analysis and to further assess in regions like the transition from tachyon dominance to fluid dominance, verifying all possible scenarios with those two tools. On the other hand, figure 2 deserves some attention when we consider the trajectories approaching the stable nodes (a)–(b) (left plot) and (f)–(g) (right plot). Therein, the trajectories approach  $x \rightarrow \pm 1$  along a segment line containing the stable nodes. This situation implies that the energy density (3.2) diverges after reaching a point where  $x \rightarrow \pm 1$ ,  $y \rightarrow 0$  and  $s \rightarrow s_1$ . This observation will be important in the next sections concerning the possible outcomes of the gravitational collapse.

## B. Analytical and numerical results

Let us herewith discuss this section possible outcomes regarding the collapsing system, employing elements from both our analytical as well of numerical study.

### 1. Tachyon dominated solutions

From the trajectories in the vicinity of (a) and (b), attractor solutions can be described.

The asymptotic behavior of  $s$  near the point (a) can be approximated as  $s \approx s_c + \exp(-\tau) = \exp(-\tau)$ ; hence, as  $\tau \rightarrow \infty$  (i.e.,  $a \rightarrow 0$ ),  $s$  vanishes. Moreover, the time derivative of the tachyon field is given by  $\dot{\phi} \simeq 1$ , that is, the tachyon field  $\phi(t)$  has a linear time dependence and can be approximated as (see figure 4)

$$\phi(t) \simeq t + \phi_0. \quad (3.24)$$

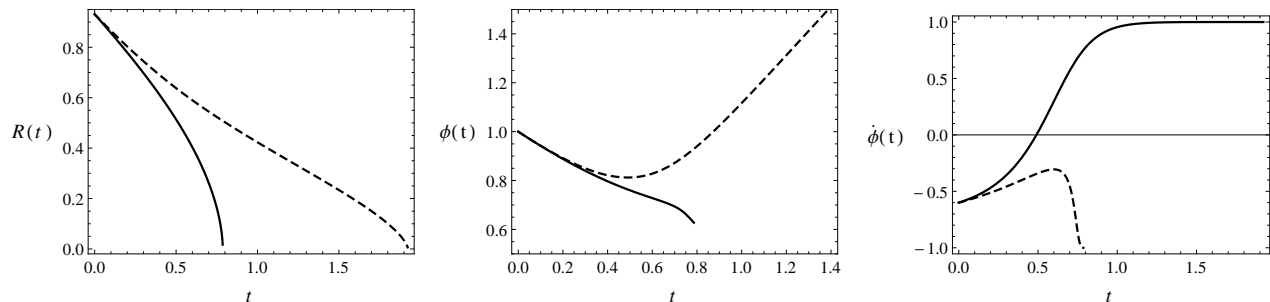


Figure 4: Behavior of the area radius, tachyon field and its time derivative over time. We considered the initial conditions as:  $t_i = 0$ ,  $\rho_{0b} = 1$ ,  $V_0 = 4/9$ ,  $a(0) = a_0$ ,  $\dot{\phi}(0) = -0.6$  and  $\phi_0 = 1$ . We also have  $\gamma = 0.1$  (full lines) and  $\gamma = 1.2$  (dashed lines).

It should be noted that, for the  $\phi > 0$  branch,  $\phi_0$  is positive on the initial configuration of the collapsing system (where  $t = 0$ ) and hence, the tachyon field increases with time, proceeding downhill the potential. Within a finite amount of time, the tachyon field reaches its maximum<sup>7</sup> but finite value  $\phi(t_s) = \phi_s$  at  $t_s < \phi_0$ , with the minimum (but non-zero value)  $V \propto \phi_s^{-2}$ . As the tachyon potential decreases, the dynamical variable  $y = \frac{V}{3H^2}$  vanishes.

Thus, as  $\dot{\phi} \rightarrow 1$ , the energy density of the system diverges. Furthermore, the tachyon pressure  $p_\phi = -V(\phi)(1 - \dot{\phi}^2)^{\frac{1}{2}}$  vanishes asymptotically<sup>8</sup> (see figure 5 for plots of the energy density, barotropic pressure and tachyon field pressure).

<sup>7</sup> The time at which the collapse reaches the singularity is finite. Thus the tachyon field at the singularity remains finite as  $\phi(t_s) = t_s + \phi_0$ .

<sup>8</sup> For the  $\phi < 0$  branch,  $\phi_0$  is negative at the initial condition. Thus, the absolute value of the tachyon field starts to decrease from the initial configuration as  $\phi(t) = t - |\phi_0|$  until the singular point at time  $t_s < |\phi_0|$ , where tachyon field reaches its minimum but non-zero value  $\phi_s$ . This leads it uphill the potential until the singular epoch, where the potential becomes maximum but finite.

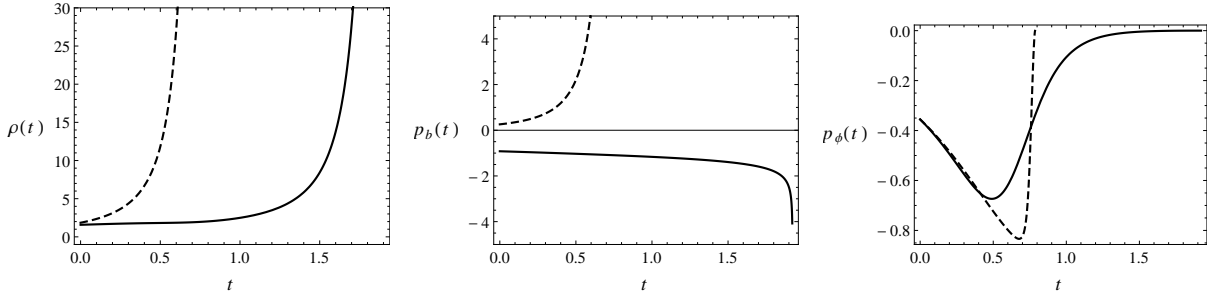


Figure 5: The energy density, barotropic pressure and tachyon field pressure. We considered  $t_i = 0$ ,  $a(0) = a_0$ ,  $V_0 = 4/9$  and  $\phi_0 = 0.6$  with  $\gamma < 1$  (full lines) and  $\gamma > 1$  (dashed lines). The total effective pressure ( $p_b + p_\phi$ ) is divergent and negative (for  $\gamma < 1$ ) in the final stage of the collapse.

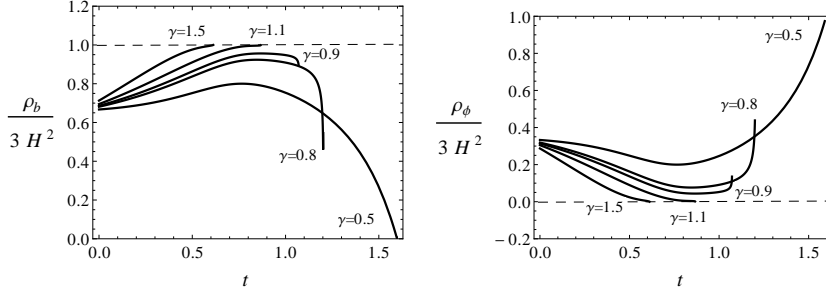


Figure 6: Behavior of the ratios  $\frac{\rho_b}{3H^2}$  (left) and  $\frac{\rho_\phi}{3H^2}$  (right). We considered the initial conditions as:  $t_i = 0$ ,  $\rho_{0b} = 1$ ,  $V_0 = 4/9$ ,  $a(0) = a_0$ ,  $\dot{\phi}(0) = -0.6$  and  $\phi_0 = 1$ . We illustrate the transition between tachyon and fluid dominated solutions as a function of the barotropic parameter. In these collapsing cases the potential does not diverge and the tachyon field does not vanish.

The total energy density of the collapsing system is given approximately by the energy density of tachyon field (see figure 6 for numerical solutions), which corresponds to a dust-like matter near the singularity as  $\rho_\phi \propto 1/a^3$ . From this relation for the tachyon energy, we may write the energy density of the system near point (a),

$$\rho \approx \rho_0 a^{-3}. \quad (3.25)$$

This induces a black hole at the collapse final state.

As far as (b) is concerned, the time dependence of the tachyon field can be obtained as

$$\phi(t) \simeq -t + \phi_0. \quad (3.26)$$

For the  $\phi > 0$  branch, the tachyon field decreases from its initial value at  $t = 0$  (where  $\phi_0 > 0$ ), moving uphill the potential. Then, the potential will reach a maximum (but finite) value when the tachyon field reaches its minimum and nonzero value (i.e.  $\phi \rightarrow \phi_s$  as  $t \rightarrow t_s \leq \phi_0$ ). In the limit case  $t_s = \phi_0$ , the tachyon field vanishes and the potential diverges. I.e.,  $y$  and  $s$  vanish, the Hubble rate increases faster than the potential and the barotropic fluid energy density diverges, that is, the total energy density of the system asymptotically diverges.<sup>9</sup> Likewise, when  $\dot{\phi} \rightarrow 1$  and  $a \rightarrow 0$ , the tachyon matter behaves as dust matter. The fate of the collapse for this fixed point is as well a black hole formation.

The asymptotic solutions provided by the fixed points (a) and (b) correspond to a dust-like solution with a vanishing pressure for the tachyon field, whose energy density reads  $\rho_\phi \propto 1/a^3$ . This is consistent with the WEC and DEC for the tachyon matter being satisfied, as was mentioned before. Concerning the status of the energy conditions for the barotropic fluid, as we indicated before, regularity of the initial data for the collapsing matter respects the WEC. On the other hand, stability of the solution in this case ensures that  $\gamma < 1$ , which satisfies the sufficient condition for the DEC.

<sup>9</sup> On the other hand, for the  $\phi < 0$  branch, the tachyon field increases from its initial condition as time evolves, proceeding to ever less negative values as  $\phi \rightarrow 0^-$ . In this case, it proceeds downhill the tachyon potential till the system reaches  $a = 0$  at  $t = t_s$ , where the Hubble rate and hence the total energy density of the system diverge. This implies that the time at which the collapse system reaches the singularity is always  $t_s \leq \phi_0$ .

## 2. Fluid dominated solutions

From the trajectories in the vicinity of  $(f)$  and  $(g)$ , solutions can be described with some having an attractor behaviour.

The asymptotic behavior of  $s$  near the point  $(f)$  can be approximated as  $s \approx 1 + \exp(-\tau)$ ; hence, as  $\tau \rightarrow \infty$  (i.e.,  $a \rightarrow 0$ ),  $s \rightarrow 1$ . Moreover, the time derivative of the tachyon field is given by  $\dot{\phi} \simeq 1$ ; that is, the tachyon field  $\phi(t)$  has a linear time dependence and can be approximated as (see figure 4),

$$\phi(t) \simeq t + \phi_0. \quad (3.27)$$

The total energy density of the collapsing system is given approximately by the energy density of the barotropic fluid (see figure 6, where  $\rho_b/(3H^2) \rightarrow 1$  while  $\rho_\phi/(3H^2) \rightarrow 0$  for  $\gamma > 1$ ), which goes, near the singularity, as  $\rho_b \propto 1/a^{3\gamma}$ . From this relation for the fluid energy, we may write the energy density of the system near point  $(f)$ ,

$$\rho \approx \rho_{0b} a^{-3\gamma}. \quad (3.28)$$

For  $\gamma < 2/3$ , the ratio  $F/R = \frac{1}{3}r^2\rho_{0b}a^{2-3\gamma}$ , converges as the singularity is reached leading to the avoidance of trapped surfaces, but since the corresponding fixed point  $(f)$  turns to be a saddle, then the resulting naked singularity is not stable. For  $2/3 < \gamma < 1$  the ratio  $F/R$  diverges and the trapped surfaces do form. But still the point  $(f)$  is saddle and the resulting black hole is not stable. The case  $\gamma > 1$  corresponds to a stable solution for which the ratio  $F/R$  goes to infinity as the collapse advances. Then, the trapped surface formation in the collapse takes place before the singularity formation and thus the final outcome is a black hole.

As far as  $(g)$  is concerned, the time dependence of the tachyon field can be obtained as

$$\phi(t) \simeq -t + \phi_0. \quad (3.29)$$

For the  $\phi > 0$  branch, the tachyon field decreases from its initial value at  $t = 0$  (where  $\phi_0 > 0$ ), moving uphill the potential, the potential will reach a maximum (but finite) value when the tachyon field reaches its minimum and nonzero value (i.e.  $\phi \rightarrow \phi_s$  as  $t \rightarrow t_s \leq \phi_0$ ). In the limit case  $t_s = \phi_0$ , the tachyon field vanishes and the potential diverges. I.e.,  $y$  and  $s$  vanish, the Hubble rate increases faster than the potential and the barotropic fluid energy density diverges, that is, the total energy density of the system, is given by equation (3.28), and asymptotically diverges. Similar to point  $(f)$  the mass function of the system for the fixed point solution  $(g)$  is given by  $F/R = \frac{1}{3}r^2\rho_{0b}a^{2-3\gamma}$ , which diverges for  $\gamma > 1$ . Therefore, the resulting singularity in this case will be covered by a black hole horizon.

As far as the energy conditions are concerned for the fixed point solutions  $(f)$  and  $(g)$ , we find that the tachyon field satisfies the WEC. Also the DEC remains valid case as well. On the other hand, for the barotropic fluid, the WEC is satisfied initially and will hold until the endstate of the collapse. The stable solution in this case corresponds to the range  $\gamma > 1$  which satisfies DEC as well.

## 3. Tracking solution: black hole and naked singularity formation

In this subsection, we will discuss a different type of solutions, where the fluid and tachyon appear with a tracking behaviour. Let us introduce this situation as follows.

Interesting and physically reasonable tracking solutions can be found, where  $\dot{\phi} \rightarrow \pm 1$ , when we consider  $\gamma \rightarrow 1$ , i.e., a situation whereby the emergence of points  $(h)$  and  $(i)$  will be of relevance as attractors. The transition from tachyon dominated to fluid dominated scenarios, like those described in previous sections, is not straightforward. In this situation, the tachyon field and barotropic fluid compete to establish the dominance in the late stage of the collapse. In figure 6 we have a illustration of this kind of solutions. The mentioned dominance seems to depend strongly on the initial ratio  $\rho_\phi/\rho_b$  at an earlier stage of the collapse and also on the value of  $\gamma$ . Such a dependence on the initial conditions can lead to a set of solutions between those provided by fixed points  $(a)$ ,  $(b)$  (tachyon dominated solutions) and by points  $(f)$ ,  $(g)$  (fluid dominated solutions). From a dynamical system point of view, this corresponds to have trajectories asymptotically approaching  $x \rightarrow \pm 1$  in sections where  $s$  is between 0 and 1 (see figure 2). At the end of the collapse we observe that  $\frac{\rho_\phi}{3H^2} \sim \frac{\rho_b}{3H^2} < 1$ , as illustrated in figure 6. Therefore, in this scenario, the trajectories would convey a collapsing case in which the energy density of the tachyon field and of the barotropic fluid are given by  $\rho_\phi \propto \rho_b \propto a^{-3\gamma}$ . This shows a tracking behavior for the collapsing system [20, 33]. Moreover, the total energy density of the collapse, in terms of  $a$ , reads

$$\rho \propto a^{-3\gamma}. \quad (3.30)$$

Equation (3.30) shows that the energy densities of the tachyon field, the barotropic matter and hence, their total (for the collapsing system), diverges as  $a \rightarrow 0$ . The ratio of the total mass function over the area radius is given by

$$\frac{F}{R} \propto \frac{1}{3} r^2 a^{2-3\gamma}. \quad (3.31)$$

Equation (3.31) subsequently implies that, for an adequate choice of values  $(\gamma, \phi_0)$ , trapped surfaces can form as the collapse evolves and a few scenarios can be extracted. More precisely, for the range  $\gamma > \frac{2}{3}$ , for both  $\phi > 0$  and  $\phi < 0$  branches, the final fate of the collapse is a black hole. For the case in which  $\gamma < \frac{2}{3}$ , the ratio  $F/R$  remains finite as the collapse proceeds and an apparent horizon is delayed or fails to form; the final state is a naked singularity (a solution for the choice of ‘-’ sign in equation (3.23)). The tracking solution indicates  $\gamma = \frac{2}{3}$  as the threshold (illustrated in figure 3), which distinguishes a black hole or a naked singularity forming.

Therefore, under suitable conditions, we can determine whether it is possible to have the formation of a naked singularity. In fact, if we assume a very unbalanced initial ratio  $\rho_\phi/\rho_b$  with  $\rho_{0\phi} \ll \rho_{0b}$  and a barotropic fluid having  $\gamma < \frac{2}{3}$ , then we can have a situation where the ratio (3.31) is converging. The set of initial conditions described by  $\rho_{0\phi} \ll \rho_{0b}$  are equivalent to consider the barotropic fluid as initially dominant. If this specific unbalanced distribution of matter is allowed to evolve into a regime where the tachyon dominates then the system will evolve until  $\rho_\phi$  becomes comparable to  $\rho_b$ . The singularity is reached in finite time and it can happen before the tachyon can effectively dominate. In figure 7 we have a graphical representation of the ratio  $F/R$ . It can be seen that the ratio  $F/R$  remains finite for  $\gamma < 2/3$ , while the energy density is diverging, as the collapse proceeds and apparent horizon is delayed or fails to form till the singularity formation. As the right plot shows, the validity of WEC is guaranteed throughout the collapse scenario for both barotropic fluid and tachyon field. Also the DEC is valid for the solutions that exhibit naked singularity, i.e., those for which  $\gamma < 2/3$ .

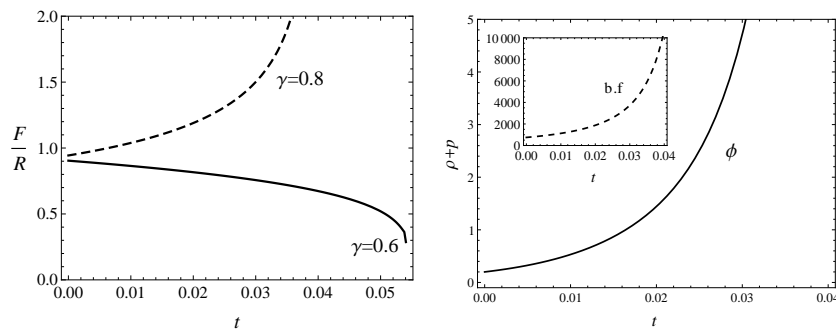


Figure 7: In the left plot it is shown the ratio of the total mass function over the area radius. We considered  $V_0 = 4/9$  and  $\rho_{0b} = 1100$ . It is shown that for  $\gamma > 2/3$  we have black formation and for  $\gamma < 2/3$  we have naked singularity formation. The right plot shows the weak energy condition over time for the barotropic fluid (b.f) and for the tachyon field ( $\phi$ ). Therein we considered  $t_i = 0$ ,  $a(0) = a_0$ ,  $V_0 = 4/9$ ,  $\frac{\rho_{0b}}{\rho_{0\phi}} = 1100$  and  $\phi_0 = 0.6$  with  $\gamma = 0.6$ .

#### 4. Other solutions

Point (c) does not represent an attractor and hence its vicinity will not corresponds to a collapse endstate. However, trajectories emerging from it would proceed towards (a) or (b). The time dependence of the tachyon field near (c) can be obtained integrating  $\dot{\phi} = -\lambda\sqrt{\frac{y_0}{3}}$  as

$$\phi(t) \simeq -\lambda\sqrt{\frac{y_0}{3}}t + \phi_0. \quad (3.32)$$

In the  $\phi > 0$  branch, the tachyon field starts to increase with time from its initial value at  $t = 0$  (where  $\phi(t = 0) = \phi_0 > 0$ ), proceeding uphill the potential. Then, a stage is obtained where a maximum (but finite) value is reached, when the tachyon field goes to its minimum and nonzero value at  $t_s \leq \lambda\sqrt{3/y_0}$ . Asymptotically,  $y = \frac{V}{3H^2} \rightarrow y_0$  and  $s = \frac{\rho_b}{3H^2} \rightarrow 0$ . Since  $y_0 > 0$  is a constant, the Hubble rate at  $t = t_s$  reads  $H = -\sqrt{V/3y_0}$  and the total energy density of the system is essentially the energy density of the tachyon field and is given by

$$\rho \equiv 3H^2 \simeq \frac{V(\phi)}{y_0}, \quad (3.33)$$

which is proportional to the tachyon potential. Therefore, at the time  $t_s < \lambda\sqrt{3/y_0}$ , when the tachyon field reaches its non-zero minimum, the total energy density of the system remains finite. In the limit case, when the time  $t_s = \lambda\sqrt{3/y_0}$ , the tachyon field vanishes, the tachyon potential diverges. Alternatively, we can also write that tachyon behaves as

$$\phi \approx a^{\frac{\lambda^2 y_0}{2}}. \quad (3.34)$$

When  $a \rightarrow 0$ , the tachyon field vanishes, and hence, the potential and energy density of tachyon field in equation (3.33), as a function of  $a$ , is given by  $\rho \propto V(\phi) \approx a^{-\lambda^2 y_0}$  and diverges at  $a = 0$ . The dynamics of the system in vicinity of this fixed point is given by  $x \approx -\frac{\lambda}{\sqrt{3}}\sqrt{y_0}$ ,  $y \approx y_0 + (a_0/a)^{3\zeta_2}$  and  $s \approx (a_0/a)^{3\zeta_3}$ , where  $\zeta_2 > 0$ .

Concerning (d), the energy density of the tachyon field is approximately given by the tachyon potential  $\rho_\phi \simeq V(\phi)$  (with  $\dot{\phi} = 0$ ) and thus, in its vicinity, the tachyon potential remains constant and finite. Furthermore,  $y = V/3H^2 \simeq 0$  and  $\rho_b/3H^2 \simeq 1$  imply that the total energy density is given by the energy density of barotropic matter only:  $\rho = 3H^2 \simeq \rho_b$ . This solution diverges as  $a \rightarrow 0$ .

The fixed point (e) for the range  $\gamma < \gamma_1$  presents solutions for the collapsing system in which  $\dot{\phi}$  asymptotically is given by  $\dot{\phi} = -\sqrt{\gamma}$ , for the  $\phi > 0$  and  $\dot{\phi} = \sqrt{\gamma}$  for the  $\phi < 0$  branch. For the  $\phi > 0$  branch, the time dependence of the tachyon field is given by

$$\phi(t) = -\sqrt{\gamma}t + \phi_0. \quad (3.35)$$

The tachyon starts its evolution from the initial configuration  $\phi_0 > 0$ , and decreases uphill the potential. Then, at the time  $t = t_s = \frac{\phi_0}{\sqrt{\gamma}}$  the tachyon field vanishes, the potential diverging<sup>10</sup>.

A thorough numerical analysis of the trajectories in the vicinity of point (e) has shown that it behaves as an unstable node. We can observe in the center plot of figure 3 an illustration of the general behavior near this point, namely having trajectories diverging from it.

### C. Exterior geometry

In order to complete the full space-time geometry for the herein collapsing model, we need to match the homogeneous interior space-time to a suitable (inhomogeneous) exterior geometry. For a perfect fluid gravitational collapse set up, with equation of state  $p = (\gamma - 1)\rho$ , the pressure does not necessarily vanish at the boundary. E.g., matching the internal geometry filled with matter (and radiation) to a boundary layer (which is crossed with the radiation), which could in turn be matched to an exterior geometry, not completely empty (e.g., filled by radiation). More concretely, matching the interior with a generalized exterior Vaidya space-time across the boundary given by  $r = r_b$  [28].

Similarly to [34], we proceed by considering the interior metric which describes the collapsing cloud as

$$ds_-^2 = -dt^2 + a^2(t)(dr^2 + r^2 d\Omega^2) \quad (3.36)$$

and the exterior one in advanced null coordinates  $(v, R)$  given by

$$ds_+^2 = -f(v, R)dv^2 + 2dv dR + R^2 d\Omega^2. \quad (3.37)$$

In these coordinates the outermost boundary of trapped surfaces is simply given by the relation  $f(v, R) = 0$ . It should be noticed that in general the formation of the singularity at  $a = 0$  is independent of matching the interior to the exterior space-time. In order to find a suitable exterior metric function  $f(v, R)$  we resort to an Hamiltonian perspective of the model. The total Hamiltonian constraint is given by [35]

$$\begin{aligned} \mathcal{H}(a, \pi_a; \pi_\phi) &= \mathcal{H}_a + \mathcal{H}_\phi + \mathcal{H}_b \\ &= \frac{\pi_a^2}{12a} + a^3 \sqrt{V^2 + a^{-6}\pi_\phi^2} + \rho_{0b} a^{-3(\gamma-1)}, \end{aligned} \quad (3.38)$$

where  $\pi_a$  and  $\pi_\phi$  are the conjugate momentums for the scale factor  $a$  and for the tachyon field  $\phi$ , respectively. Furthermore, the Hamilton equations for parameters  $a$ ,  $\pi_a$  and  $\pi_\phi$  can be obtained by using the equation (3.38) as

<sup>10</sup> For the  $\phi < 0$  branch, the time dependence of the tachyon field is given by  $\phi(t) = \sqrt{\gamma}t + \phi_0$ . Therefore the tachyon field starts its evolution from the initial configuration at  $\phi_0 < 0$ , decreasing in time, going uphill the potential.

follows:

$$\dot{a} = \frac{\partial \mathcal{H}}{\partial \pi_a} = \frac{\pi_a}{6a}, \quad \dot{\phi} = \frac{\partial \mathcal{H}}{\partial \pi_\phi} = \frac{a^{-3}\pi_\phi}{\sqrt{V^2 + a^{-6}\pi_\phi^2}}, \quad (3.39)$$

$$\dot{\pi}_a = -\frac{\partial \mathcal{H}}{\partial a} = \frac{\pi_a^2}{12a^2} + 3(\gamma - 1)\rho_{0b}a^{-(1+3(\gamma-1))} - \frac{3a^5V^2}{\sqrt{a^6V^2 + \pi_\phi^2}}, \quad (3.40)$$

$$\dot{\pi}_\phi = -\frac{\partial \mathcal{H}}{\partial \phi} = -\frac{a^3VV_{,\phi}}{\sqrt{a^6V^2 + \pi_\phi^2}}, \quad (3.41)$$

On the other hand, since the Hamiltonian constraint,  $\mathcal{H} = 0$ , must be held across the boundary  $\Sigma$ , equation (3.38) reduces to

$$\pi_\phi^2 = \frac{\pi_a^4}{144a^2} + \rho_{0b}^2a^{-6(\gamma-1)} + \rho_{0b}\frac{\pi_a^2a^{-3(\gamma-1)}}{6a} - a^6V^2, \quad (3.42)$$

whereby, substituting for  $\pi_a$  and  $\pi_\phi$  from equation (3.39)-(3.41), we get

$$9a^2\dot{a}^4 + \rho_{0b}^2a^{-6(\gamma-1)} + 6\rho_{0b}\dot{a}^2a^{2-3\gamma} = \frac{a^6V^2}{1 - \dot{\phi}^2}. \quad (3.43)$$

Furthermore, it is required for the junction condition  $r_b a(t) = R(t)$  and the equation of motion for scale factor  $r_b \dot{a} = \dot{R}$  to be satisfied at the boundary of two regions. By substituting these conditions in the Hamiltonian constraint equation,  $\mathcal{H}(v, R) = 0$ , given by (3.43), we get

$$(1 - f) \left[ 9(1 - f) + 6\rho_{0b} \left( \frac{R}{r_b} \right)^{4-3\gamma} \right] = \left( \frac{R}{r_b} \right)^4 \left[ \frac{V^2}{1 - \dot{\phi}^2} - \rho_{0b}^2 \left( \frac{R}{r_b} \right)^{-6\gamma} \right], \quad (3.44)$$

Notice that, we have substituted the four-velocity of the boundary being seen from the exterior by  $\dot{R} = -\sqrt{1-f}$  (cf. [34]). Then, by solving equation (3.44) for  $f$ , the boundary function is obtained simply as

$$f(R) = 1 - \frac{2}{3} \frac{V}{\sqrt{1 - \dot{\phi}^2}} \left( \frac{R}{r_b} \right)^2 + \frac{1}{3} \rho_{0b} \left( \frac{r_b}{R} \right)^{1+3(\gamma-1)}. \quad (3.45)$$

Let us now study the behavior of the boundary function for the stable fixed point solutions we obtained in the previous subsections. We note that the above expression is valid when both the tachyon field and barotropic fluid are present, thus in the regimes where the tachyon field is dominant the contribution of the fluid to Hamiltonian constraint is set aside. For the dust-like solutions, described by points (a) and (b), the energy density of tachyon field at the boundary  $r_b$ , included in second term of equation (3.45), is given by  $\rho_\phi \approx \rho_o r_b^3 / R^3$ . So, the boundary function  $f$  in equation (3.45) reduces to:

$$f(R) = 1 - \frac{M}{R}, \quad \text{where} \quad M \equiv \frac{4\pi}{3} r_b^3 \tilde{\rho}_o, \quad (3.46)$$

and  $\tilde{\rho}_o \equiv \rho_o / 2\pi r_b^2 = \text{const}$ . Equation (3.46) for  $f(R)$  constrains the exterior space-time to have a Schwarzschild metric in advanced null coordinates, providing an interpretation of the collapsing system as a dust ball with the radius  $r_b$  and the density  $\tilde{\rho}_o$ . On the other hand, for the fixed point solution (e), by using the equation (3.30) in (3.45), we have

$$f(R) = 1 - \frac{\tilde{M}}{R^{3\gamma-2}}, \quad \text{where} \quad \tilde{M} \equiv \frac{2}{3} \left( \rho_0 - \frac{2s_0 + 1}{s_0} \rho_{0b} \right) r_b^{3\gamma-2} = \text{const}, \quad (3.47)$$

where  $3\gamma - 2 > 0$  (notice that, this corresponds to the case in which  $\gamma = \gamma_1 > 2/3$  in previous subsection).

In order to get a possible class of dynamical exterior solutions, we proceed by considering the following metric at the boundary [34]

$$ds^2 = - \left( 1 - \frac{2M(R, v)}{R} \right) dv^2 + 2dv dR + r^2 d\Omega^2, \quad (3.48)$$

where

$$M(R, v) = m(v) - \frac{g(v)}{2(2\gamma - 3)R^{2\gamma-3}}, \quad (3.49)$$

is the total mass within the collapsing cloud. Matching the for exterior metric function gives

$$\begin{aligned} 1 - \frac{2m(v)}{R} + \frac{g(v)}{(2\gamma - 3)R^{2\gamma-2}} &= 1 - \frac{\tilde{M}}{R^{3\gamma-2}}, \\ \frac{2\dot{m}(v)}{R} &= \frac{\dot{g}(v)}{(2\gamma - 3)R^{2\gamma-2}}, \end{aligned} \quad (3.50)$$

in which, the second part stands for matching for the extrinsic curvature. Differentiation of the first expression in (3.50) with respect to time and using the second one, we get

$$\frac{2m(v)}{R^2} - \frac{2(\gamma - 1)g(v)}{(2\gamma - 3)R^{2\gamma-1}} = \frac{\tilde{M}(3\gamma - 2)}{3R^{3\gamma-1}}. \quad (3.51)$$

Multiplying the first expression in equation (3.50) by  $R^{-1}$  and after adding the result with the above equation, we get

$$g(v) = -\frac{\tilde{M}(\gamma - 1)}{R(v)^\gamma}. \quad (3.52)$$

Now, by substituting for  $g(v)$  into equation (3.50), we obtain

$$m(v) = \frac{\tilde{M}\gamma}{6(3 - 2\gamma)R(v)^{3\gamma-3}}. \quad (3.53)$$

Then, as seen from equation (3.31) for  $\gamma < 2/3$ , where the trapping of light has failed to occur, the exterior geometry is dynamical in contrast to the tachyon dominated regime in which a space-like singularity forms with a static exterior space-time. Finally, for fluid dominated solutions, depending on the value of  $\gamma$ , both naked singularities and black holes may form, the mass being different to those of tracking solutions and the exterior geometry being static or dynamical, respectively.

#### IV. CONCLUSIONS, DISCUSSION AND OUTLOOK

In this paper we considered a particular setting among the spherically symmetric class of models for gravitational collapse, with a tachyon field and a barotropic fluid as matter content. We restricted ourselves to the marginally bound case (cf. [1, 21, 36] for a description and details). The tachyon potential was assumed to be of an inverse square form. Our objective was to establish (i) which final states would occur (namely, a black hole or a naked singularity), (ii) how each matter component will compete (the fluid being conventional, whereas the tachyon bringing some workable but intrinsic non-standard effects from string theory) and, (iii) which will eventually be the determinant component at the end of the collapse process. More precisely, in our opinion it is of interest to assert, if and how, at later stages, effects induced by the tachyon (a scalar field (among others) found in string theory context), could allow interesting features to be eventually discussed (i.e., what asymptotic behaviour emerges). As far as the tachyon field is concerned, from eq. (3.4) we can have that with  $-1 < \dot{\phi} < 1$  and  $H < 0$ ,  $\dot{\phi}$  terms act like an anti-friction contribution at a collapsing phase, within an uphill evolution for the  $\phi^{-2}$  potential for tachyon field (i.e., when  $\dot{\phi} < 0$ ). Moreover, other terms (i.e. the term including  $\frac{V_{,\phi}}{V}$ ) would have an anti-friction effect as well.

Determining therefore the outcome of the gravitational collapse in our system<sup>11</sup>, i.e., whether, e.g., a black hole or naked singularity would form, was not a straightforward assessment. We considered an analytical description by means of a phase space analysis [20, 32], discussing several asymptotic behaviours; these were also subject to a careful study involving a numerical investigation, which added a clearer description of the possible dynamical evolutions.

---

<sup>11</sup> The case of a standard scalar field was investigated in [21, 36]

Within this setting, for a spatially homogeneous interior space-time, we found a situation where the tachyon was dominant, with a black hole forming<sup>12</sup>. A cosmological framework involving only a FRW geometry, with a tachyon field and a barotropic fluid, was investigated in [20], focusing on the late time (dark energy like) stages. It is interesting to note that while for a tachyon dominated regime, an inflationary-like (i.e., accelerated expansion) scenario leads to violation of the strong energy condition (SEC)<sup>13</sup> [20], in our collapse scenario we have instead a corresponding asymptotic stage, where tachyon dominance leads to black hole formation, satisfying the SEC at the final state of the collapse (cf. figure (4)). The same behaviour is observed in the fluid dominated regime, where for  $\gamma > 1$  the SEC is satisfied by the fluid, with a black hole formation. However, for the tracking solutions, where a naked singularity forms, i.e.,  $\rho_{0b} \gg \rho_{0\phi}$  and  $\gamma < 2/3$ , the SEC is violated.

Moreover, in further comparison with the set of fixed points found in [20] for an expanding (accelerating) universe ( $H > 0$ ), we have found analytically two additional critical points ( $f$  and  $g$ ) for the collapse process which correspond to a barotropic dominated collapsing regime which ends in a black hole for  $\gamma > 1$ , respecting the WEC and SEC. Indeed, for the late-time acceleration of the universe, filled with a tachyon field and a fluid, the phase space analysis in [20] predicted two class of solutions: a tachyon dominated solution; and a tracking solution [20]. Rather differently, corresponding solutions herein our paper turn to be unstable towards the singularity in the collapse process. Nevertheless, two other solutions are also provided in our collapsing scenario: a tachyon dominated solution where  $\gamma$  satisfies the range  $\gamma < 1$ , initially; and a barotropic dominated solution for which the barotropic parameter holds the range  $\gamma > 1$ . All these solutions predict a black hole formation as collapse end state.

Further regarding the tracking solutions (of a cosmological nature) indicated in [20]. In our collapsing system, a different and rather interesting set of states is found, within the context of tracking behavior for the barotropic fluid plus tachyon field content. Being more concrete, these solutions have that a black hole or naked singularity forms. In particular, in this situation, we found that it is possible to define by a numerical appraisal in particular, the threshold  $\gamma = 2/3$ , separating black hole and naked singularity solutions for the gravitational collapse. We have also discussed the specific conditions leading to the formation of a naked singularity. Therefore, we concluded, that in our model, if the collapse starts with an unbalanced distribution of the matter content favoring the barotropic fluid, i.e.  $\rho_\phi \ll \rho_b$ , then towards the final stage of the collapse they evolve until  $\rho_\phi \approx \rho_b$ , when a naked singularity forms. However, since the NEC is satisfied, the strong curvature condition along the null geodesics can be preserved and the singularity can be strong in the sense of [37].

We think it is fair to indicate that we employed a  $\phi^{-2}$  potential for the tachyon, whereas for  $\phi \rightarrow 0$ , the tachyon should not induce a divergent behavior as far as string theory advises [38–42]. In fact, an exponential-like potential for the tachyon could bring a richer set of possible outcomes [29, 38, 43, 44], including a better behaved and possibly a more realistic evolution when dealing with  $\phi \rightarrow 0$ .

Finally, let us add that it will be of interest to investigate (i) other scenarios for the geometry of the interior space-time region, (ii) specific couplings between the tachyon and the fluid, within e.g., a chameleon scenario for gravitational collapse and black hole production (broadening the scope in [45–47]), (iii) adding either axionic, dilatonic or other terms (e.g., curvature invariants) that could be considered from a string setup, but at the price of making the framework severely less workable and (iv) whether explicit quantum effects can alter the outcomes presented in this paper. To this purpose latter, we plan to use ingredients brought from loop quantum gravity (cf. ref. [48]).

## V. ACKNOWLEDGMENTS

The authors would like to thank P. Joshi, A. Khaleghi, C. Kiefer, F. C. Mena, A. Vikman, and J. Ward for making useful suggestions and comments. They are also grateful to the referee for the useful comments and suggestions on the issue of energy conditions. YT is supported by the Portuguese Agency Fundação para a Ciência e Tecnologia through SFRH/BD/43709/2008. This research work was also supported by the grant CERN/FP/109351/2009 and CERN/FP/116373/2010.

---

[1] P. Joshi, *Gravitational Collapse and Space-Time Singularities*, (Cambridge University Press, 2007).

<sup>12</sup> It is worthwhile to compare the result obtained herein for a homogeneous (tachyonic) collapsing matter field with the gravitational collapse of a k-essence scalar field with non-standard kinematic terms in [30], where the scalar field has a dependence to the radius  $r$  i.e.,  $\phi = \phi(r)$ . In both models, the collapsing systems lead to the black hole formation.

<sup>13</sup> Satisfying the SEC for the tachyon field demands that  $\rho_\phi + 3p_\phi \geq 0$ . Thus, the SEC holds if  $\dot{\phi}^2 > 2/3$ .



- [2] S. W. Hawking, G. F. R. Ellis, *The Large Scale Structure of Space-Time*, (Cambridge University Press, 1974).
- [3] R. Penrose, Riv. Nuovo Cimento **1** 252 (1969).
- [4] T. Harada, Phys. Rev. D **58** (1998) 104015;  
T. Harada and H. Maeda, Phys. Rev. D **63** (2001) 084022;  
R. Goswami and P. S. Joshi, Class. Quantum Grav **19** (2002) 5229;  
R. Giambò, F. Giannoni, G. Magli and P. Piccione, Gen. Rel. Grav **36** (2004) 1279;  
J. F. Villas da Rocha and A. Wang, Class. Quantum Grav **17** (2000) 2589;  
R. Giambò, F. Giannoni, G. Magli and P. Piccione, Class. Quantum Grav **20** (2003) 4943.
- [5] P. Szekeres and V. Iyer, Phys. Rev. D **47** (1993) 4362;  
S. Barve, T. P. Singh, and L. Witten, Gen. Rel. Grav. **32** (2000) 697;  
A. A. Coley and B. O. J. Tupper, Phys. Rev. D **29** 2701 (1984);  
K. Lake, Phys. Rev. D **26** (1982) 518.
- [6] R. Giambò, Class. Quantum Grav **22** (2005) 2295;  
S. Bhattacharya, R. Goswami and P. S. Joshi, Int. J. Mod. Phys. D **20** (2011) 1123;  
S. Bhattacharya, arXiv:1107.4112 [gr-qc].
- [7] A. Ori and T. Piran, Phys. Rev. Lett **59** (1987) 2137;  
A. Ori and T. Piran, Phys. Rev. D **42** (1990) 1068;  
T. Foglizzo and R. Henriksen, Phys. Rev. D **48** (1993) 4645.
- [8] F. C. Mena, B. C. Nolan and R. Tavakol Phys. Rev. D **70** (2004) 084030;  
S. G. Gosh and N. Dadhich, Gen. Rel. Grav. **35** (2003) 359;  
T. Harko, S. K. Cheng, Phys. Lett. A **226** (2000) 249.
- [9] C. Gundlach and J. M. Martín-García, Living Rev. Relativity **10** (2007), 5.  
F. E. Schunck and E. W. Mielke, Class. Quant. Grav. **20** (2003) R301; arXiv:0801.0307 [astro-ph].
- [10] R. Giambò, F. Giannoni and G. Magli, J. Math. Phys. **49** (2008) 042504; Gen. Rel. Grav. **41** (2009) 21.
- [11] K. Ganguly and N. Banerjee, Gen. Rel. Grav. **43** (2011) 2141.
- [12] A. I. Janis, E. T. Newman and J. Winicour, Phys. Rev. Lett **20** (1968) 878;  
M. Wyman, Phys. Rev. D **24** (1981) 839;  
B. C. Xanthopoulos and T. Zannias, Phys. Rev. D **40** (1989) 2564;  
O. Bergmann and R. Leipnik, Phys. Rev. **107** 1157 (1957);  
H. A. Buchdahl, Phys. Rev **115** (1959) 1325.
- [13] M. Choptuik, Phys. Rev. Lett. **70** (1993) 9.
- [14] D. Christodoulou, Ann. Math. **140** (1994) 607.
- [15] F. I. M. Pereira and R. Chan, Int. J. Mod. Phys. D **17** (2008) 2143; arXiv:0803.2628 [gr-qc].
- [16] M. Jankiewicz and A. A. Sen, arXiv:0602.085 [gr-qc].
- [17] A. Mazumdar, S. Panda and A. Perez-Lorenzana, Nucl. Phys. B **614** 101 (2001).
- [18] Yun-Song Piao, Rong-Gen Cai, Xinmin Zhang, and Yuan-Zhong Zhang, Phys. Rev. D **66** (2002) 121301;  
M. Fairbairn and M. H. G. Tytgat, Phys. Lett. B **546** 1 (2002).
- [19] A. Sen, Int. J. Mod. Phys. A, **20** (2005) 5513; arXiv: 0410.103 [hep-th].
- [20] Juan M. Aguirregabiria and Ruth Lazkoz, Phys. Rev. D **69**, 123502 (2004).
- [21] R. Goswami, P. Joshi and P. Singh, Phys. Rev. Lett. **96**, 031302 (2006).
- [22] S. A Hayward, Phys. Rev. D **53**, 1938 (1996);  
C. W. Misner and D. H. Sharp, Phys. Rev. **136**, B571 (1964);  
D. Bak and S. J. Rey, Class. Quantum Grav. **17**, L83 (2000).
- [23] T. P. Singh, Phys. Rev. D **58**, 024004 (1998).
- [24] E. Malec, N. Ó Murchadha, Phys. Rev. D **47**, 1454 (1993).
- [25] R. Goswami, and P. Joshi, [arXiv: 0410.144 [gr-qc] (2004).
- [26] A. H. Ziaie, K. Atazadeh and Y. Tavakoli, Class. Quant. Grav. **27**, 075016 (2010); arXiv: 1003.1725 [gr-qc];  
A. H. Ziaie, K. Atazadeh, S. M. M. Rasouli (2011), arXiv: 1106.5638 [gr-qc].
- [27] P. S. Joshi and R. Goswami, Class. Quantum Grav. **24** 2917 (2007);  
R. Goswami, P. S. Joshi, C. Vaz and L. Witten, Phys. Rev. D **70** 084038 (2004);  
P. S. Joshi and R. Goswami, arXiv:0711.0426v1 [gr-qc]
- [28] P. S. Joshi and I. H. Dwivedi, Class. Quant. Grav, **16** 41 (1999); A. Wang and Y. Wu, Gen. Relat. Grav, **31** 107 (1999).
- [29] Mohammad R. Garousi, Nucl. Phys. B **584**, 284 (2000); E. A. Bergshoeff, M. de Roo, T.C. de Wit, E. Eyras, S. Panda, J. High Energy Phys. **05**, 009 (2000).
- [30] R. Akhoury, D. Garfinklea, and R. Saotomea, J. high Energy Phys. **1104**, 096 (2011); arXiv: 1103.0290 [gr-qc].
- [31] Andrei Frolov, Lev Kofman, Alexei Starobinsky, Phys. Lett. B **545** 8 (2002); arXiv: 0204187 [hep-th].
- [32] H. K. Khalil, *Nonlinear Systems*, 2nd edition (Englewood Cliffs. NJ: Prentice Hall, 1996); Jack Carr, *Applications of Center Manifold Theorem* (Springer-Verlag, 1981); J. Guckenheimer, P. Holmes, *Nonlinear Oscillations, Dynamical Systems and Bifurcation of Vector Fields* (Springer-Verlag, 1983).
- [33] A. R. Liddle, and R. J. Scherrer, Phys. Rev. D **59**, 023509 (1999).
- [34] B. K. Tippett and V. Hussain, Phys. Rev. D **84** (2011) 104031.
- [35] A. A. Sen Phys. Rev. D **74** 043501 (2006); M. Tsamparlis and A Paliathanasisa, arXiv:1111.5567 [gr-qc].
- [36] R. Goswami, and P. Joshi, arXiv: 0410.144 [gr-qc].

- [37] F. J. Tipler, Phys. Lett. A **67** (1977) 8; F. J. Tipler, C. J. S. Clarke, and G. F. R. Ellis, in General Relativity and Gravitation, edited by A. Held (Plenum, New York, 1980), vol. 2, p. 97; C. J. S. Clarke, The Analysis of Space-time Singularities (Cambridge University Press, Cambridge, England, 1993).
- [38] A. Feinstein, Phys. Rev. D **66**, 063511 (2002).
- [39] Z-K. Guo, Y. S. Piao, R. G. Cai, and Y. Z. Zhang, Phys. Rev. D **68**, 043508 (2003).
- [40] L. R. W. Ambramo and F. Finelli, Phys. Lett. B **575**, 165 (2003).
- [41] E. J. Copeland, M. R. Garousi, M. Sami, and S. Tsujikawa, Phys. Rev. D **71**, 043003 (2005).
- [42] I. Quiros, T. Gonzalez, D. Gonzalez, Y. Napoles, R. García-Salcedo, and C. Moreno, Class. Quant. Grav. **27**, 215021 (2010).
- [43] A. Sen, J. High Energy phys. **12**, 021 (1998).
- [44] A. A. Sen, J. high Energy Phys. **04**, 048 (2002); A. A. Sen, J. high Energy Phys. **07**, 065 (2002); **16**, 281 (1989); S. H. Ghate, R. V. Saraykar, and K. D. Patil, Pramana, J. Phys. **53**, 253 (1999).
- [45] V. Folomeev, arXiv:1205.2974 [astro-ph].
- [46] V. Folomeev and D. Singleton, Phys. Rev. D **85** (2012) 064045; arXiv:1112.1786 [astro-ph].
- [47] V. Folomeev, Phys. Rev. D **85** (2012) 024008; arXiv:1108.3395 [astro-ph].
- [48] Yaser Tavakoli, João Marto, Amir Hadi Ziaie and Paulo Vargas Moniz, *Semiclassical gravitational collapse with tachyon field and barotropic fluid*, to appear in PRD (2013).